

IMPROVED FAST-ICA ALGORITHM BASED ON CONVERGENCE PROOF OF NONLINEAR FUNCTION

Pengfei XU¹, Yinjie JIA^{1,2}, Zhijian WANG¹, Mingxin JIANG²

¹ College of Computer and Information, Hohai University, Nanjing, Jiangsu 210098, China

² Faculty of Electronic Information Engineering, Huaiyin Institute of Technology, Huaian, Jiangsu 223003, China

Corresponding author: Yinjie JIA, E-mail: jiayinjie@hhu.edu.cn

Abstract. The selection of nonlinear function has a significant influence on the separation performance of Fast-ICA. This paper proves the convergence performance of the sine function as a Fast-ICA nonlinear function. The simulation results show that the proposed algorithm is suitable for an image signal, communication signal, sound signal, and linear frequency modulated signal. Furthermore, the performance of the algorithm according to the increase of the number of sources is analyzed.

Key words: fast-ICA, nonlinear function, convergence.

1. INTRODUCTION

Blind source separation (BSS) is a problem of recovering or estimating unknown multiple sources from a given set of mixed or observed mixtures captured by the receiving end of the detector. BSS has wide applications in various areas such as speech recognition, telecommunications, image processing, fault diagnosis, and biomedical signal processing.

The linear model of the basic instantaneous BSS can be mathematically expressed in the vector form as follows [1]:

$$\mathbf{x}(t) = \mathbf{A} \mathbf{s}(t), \quad (1)$$

where \mathbf{A} is an unknown $m \times n$ mixing matrix which order is $m \times n$, $\mathbf{s}(t) = [s_1(t) \cdots s_n(t)]^T$ is an unknown source signal vector which order is $n \times 1$, $\mathbf{x}(t) = [x_1(t) \cdots x_m(t)]^T$ is a known mixed signal vector which order is $m \times 1$.

Independent component analysis (ICA) is the most commonly used instantaneous blind source separation algorithms. In ICA, the aim is to process the known mixed signal $\mathbf{x}(t)$ and extract a set of statistically independent vectors $\mathbf{y}(t)$. ICA seeks an unknown demixing matrix or separating matrix \mathbf{W} which order is $n \times m$, the general solution of the BSS problem can be expressed in the vector form as follows:

$$\mathbf{y}(t) = \mathbf{W} \mathbf{x}(t), \quad (2)$$

where $\mathbf{y}(t) = [y_1(t) \cdots y_n(t)]^T$ is the recovered or separated signal vector which order is $n \times 1$.

As an essential variant of the ICA algorithm, the fast independent component analysis (Fast-ICA) has been studied and widely used to solve many blind source separation problems. It is a fixed-point training algorithm based on the non-Gaussian characteristics of the source signal, providing a fast convergence speed. In 1997, Hyvarinen first proposed the Fast-ICA algorithm based on kurtosis [2]. Kurtosis is a non-Gaussian measure, but it is easily affected by individual outliers and has high sensitivity. Also, another non-Gaussian measure, the negative entropy, was used as an objective function in [3]. In this method, the blind source separation was conducted by maximizing the negative entropy indicating the strongest degree of the non-Gaussian in the separated signal.

The performance and efficiency of the negative entropy-based Fast-ICA depend on the selection of nonlinear function $g(\cdot)$. In the existing methods, the following three nonlinear functions are most commonly used [3]

$$\begin{cases} g_1(y) = \tanh(y) \\ g_2(y) = y \exp(-y^2 / 2) \\ g_3(y) = y^3 \end{cases} \quad (3)$$

$g_1(\cdot)$ is suitable for the coexistence of super-Gaussian and sub-Gaussian signals, $g_2(\cdot)$ is suitable for super-Gaussian signals, and $g_3(\cdot)$ is suitable for sub-Gaussian signals.

In practical application, the selection of nonlinear function of the Fast-ICA is varied according to the non-Gaussian characteristics of the source signal. In order to overcome this inconvenience, a new nonlinear function was proposed in [4]. However, the method was not sufficiently proved experimentally and descriptively. The motivation of the present study is to compensate for the weakness and intends to prove the stability of the sine function as a nonlinear function across different types of signals, including image signal, communication signal, sound signal, and LFM signal.

The major contribution of this paper is proving the convergence of the new nonlinear function in the Fast-ICA algorithm. The remainder of this paper is organized as follows: Section 2 describes the basis of nonlinear function selection and proves the convergence. Section 3 verifies the effectiveness of the algorithm through simulation experiments. Section 4 concludes this paper.

2. METHODOLOGY

2.1. Selection of nonlinear function

This section describes the superiority of the sine function, $g_4(u) = \sin(u)$, as the Fast-ICA nonlinear function from three aspects:

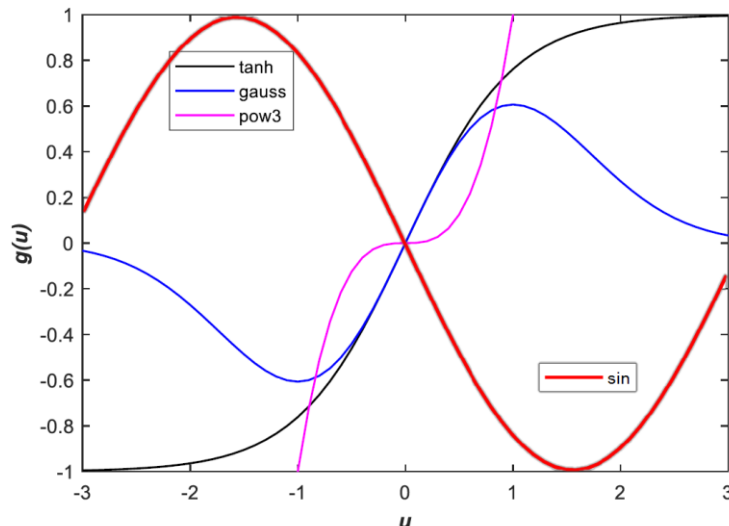


Fig. 1 - Four nonlinear functions.

(1) Figure 1 shows the four nonlinear functions: $g_1(u)$, $g_2(u)$, $g_3(u)$, and $g_4(u)$. $g_1(u)$, $g_2(u)$, and $g_3(u)$ are labeled as 'tanh,' 'Gauss,' and 'pow3', respectively. The proposed sine function $g_4(u)$ is labeled as 'sin'. As shown in Fig. 1, all four nonlinear functions have the shape characteristics of parity and symmetry. From the point of view of function image property, it is reasonable to choose $g_4(u)$.

(2) $g_4(u)$ does not require complex operations such as exponent, logarithm, and high power. Also, it does not depend on the setting range of parameters, which can improve the robustness of the Fast-ICA algorithm.

(3) $g_4(u)$ satisfies the convergence condition $E\{s_i g(s_i) - g'(s_i)\} > 0$ (resp. < 0) of the Fast-ICA algorithm [5,6].

Proof of (3). For any non-Gaussian source signal s_i , there is always a value range of $[-\theta, \theta]$, which makes the

$$E\{s_i g(s_i) - g'(s_i)\} \neq 0. \quad (4)$$

① For the convenience of substitution, $g_4(u)$ is recorded as g here. Under certain conditions, inequality (4) is actually consistent with the assumption that the source signal is non-Gaussian. In order to explain the conclusion, the left part of inequality (4) is computed by partial integration, as follows:

$$\begin{aligned} E\{s_i g(s_i) - g'(s_i)\} &= \int_{-\infty}^{\infty} (s g(s) - g'(s)) \phi(s) ds = \int_{-\infty}^{\infty} s g(s) \phi(s) ds - \int_{-\infty}^{\infty} g'(s) \phi(s) ds = \\ &= \int_{-\infty}^{\infty} s g(s) \phi(s) ds - \int_{-\infty}^{\infty} \phi(s) dg(s) = \int_{-\infty}^{\infty} s g(s) \phi(s) ds - (\phi(s) g(s)) \Big|_{-\infty}^{\infty} - \int_{-\infty}^{\infty} g(s) d\phi(s) \\ &= \int_{-\infty}^{\infty} s g(s) \phi(s) ds + \int_{-\infty}^{\infty} g(s) d\phi(s) - \phi(s) g(s) \Big|_{-\infty}^{\infty}. \end{aligned}$$

If s_i is a Gaussian distribution, then $\phi(s) = \frac{e^{-s^2/2}}{\sqrt{2\pi}}$ and $d\phi(s) = -s\phi(s)$, thus, the first two terms are canceled.

Since $G(s)$ is an even function, the derivative $g(s)$ of $G(s)$ is an odd function. Because the odd function multiplied by the even function results in the odd function, $\phi(s)$ is an even function. Accordingly, $\phi(s)g(s)$ is an odd function. If $\phi(s)g(s)$ is integrated on the symmetric interval $[-\theta, \theta]$, then $\int_{-\theta}^{\theta} g(s)\phi(s)ds = 0$.

② Without loss of generality, it is assumed that the probability density function $p(s)$ of the source signal s is a symmetric even function. When $p(s)$ is asymmetric, it can be transformed into symmetric distribution by symmetric transformation $p(s) \rightarrow \frac{p(s) + p(-s)}{2}$. First, the left part of the inequality is computed.

$$E\{s_i g(s_i) - g'(s_i)\} = \int_{-\infty}^{\infty} (s \cdot g(s) - g'(s)) p(s) ds = \int_{-\infty}^{\infty} (s \cdot \sin(s) - \cos(s)) p(s) ds. \quad (5)$$

Here we define $F(s, \theta) = E\{s g(s) - g'(s)\}$ and use the counter-proof method: the hypothesis that inequality (4) does not hold, which means that equation (5) holds for all θ .

$$F(s, \theta) = \int_{-\theta}^{\theta} (s \cdot \sin(s) - \cos(s)) p(s) ds = 0. \quad (6)$$

In the interval $[-\theta, \theta]$, s is an odd function, $\sin(s)$ is an odd function, $\cos(s)$ is an even function, and $p(s)$ is an even function. Because an odd function multiplied by an odd function results in an even function, $s \cdot \sin(s)$ is an even function. Since an even function plus or minus an even function is an even function, $s \cdot \sin(s) - \cos(s)$ is an even function. Since an even function multiplied by an even function equals an even function, $(s \cdot \sin(s) - \cos(s)) p(s)$ is an even function.

Let $f(s) = (s \cdot \sin(s) - \cos(s))p(s)$, then $F(s, \theta) = \int_{-\theta}^{\theta} f(s)ds = 2 \int_0^{\theta} f(s)ds = 0$. Obviously, for all θ , the integral $\int_0^{\theta} f(s)ds$ of the non-zero function $f(s)$ can not always be zero. Therefore, the hypothesis does not hold. That is to say, for any non-Gaussian source signal, there is always an interval $[-\theta, \theta]$, which makes inequality (4) hold.

2.2. The improved algorithm

The Fast-ICA algorithm based on nonlinear function g_4 , Fast-ICA(sin), aims to improve the robustness of the Fast-ICA algorithm further. Let denote the number of source signals be n and the number of observation signals be p , where $p \geq n$. The number of source signals will affect the separation performance of the Fast-ICA(sin) algorithm, the separation performance decreases as the number of source signals increases (for details, please refer to the conclusion of simulation 2 in section 3).

The source signal is assumed to be independent and identically distributed (i.i.d.) and non-Gaussian. The Fast-ICA (sin) algorithm is conducted as described in Table 1.

Table 1
Steps of Fast-ICA(sin) algorithm

Input: The mixed signals \mathbf{X} .
Output: The separation matrix \mathbf{W} .
Step 1: Whiten the mixed signals \mathbf{X} , namely $E(\mathbf{X}_i) = 0$ and $E(\mathbf{X}^T \mathbf{X}) = \mathbf{I}$.
Step 2: Update the nonlinear function $g_4(u) = \sin(u)$.
Step 3: Initialize the number of estimated vectors, Let $p = 1$.
Step 4: Initialize \mathbf{w}_p , namely $\mathbf{w}_p = \mathbf{w}_p / \ \mathbf{w}_p\ $.
Step 5: $\mathbf{w}_p = E\{\mathbf{X} g(\mathbf{w}_p^T \mathbf{X})\} - E\{g'(\mathbf{w}_p^T \mathbf{X})\} \mathbf{w}_p$.
Step 6: $\mathbf{w}_{p+1} = \mathbf{w}_{p+1} - \sum_{j=1}^p \mathbf{w}_{p+1}^T \mathbf{w}_j \mathbf{w}_j$.
Step 7: If $ \mathbf{w}_{p+1} - \mathbf{w}_p < \varepsilon$, return to Step 5. Otherwise, go Step 8.
Step 8: Let $p = p + 1$, if $p < n$, return to Step 3. Otherwise, the algorithm ends.

The algorithm in Table 1 differs from the original Fast-ICA algorithm only in the second step, that is, the three commonly used nonlinear functions $g_1(\cdot)$, $g_2(\cdot)$ or $g_3(\cdot)$ in equation (3) can be replaced by the proposed nonlinear function $g_4(\cdot)$.

3. EXPERIMENTS AND RESULTS

In order to verify the theoretical proof and Fast-ICA(sin) algorithm in Section 2, the simulation experiment of mixed blind separation in this section is conducted for music signals, image signals, communication signals, and linear frequency modulated (LFM) signals. Let denote the mixed matrix \mathbf{A} be a random matrix, where its elements are evenly distributed in the interval (0,1).

The separation performance of the Fast-ICA(sin) algorithm is verified in terms of the average correlation coefficient and average running time [4]. The experiments were conducted in the same hardware and software environments (Experimental Platform: MATLAB 2017b, Operating System: 64-bit Windows 7, CPU: Intel® Core™ i7-2720QM Processor @2.20GHz, and RAM: 16 GB) for each Fast-ICA algorithm under different nonlinear functions, ensuring fair comparison. The download link of the original Fast-ICA program can be obtained from the URL: <http://research.ics.aalto.fi/ica/fastica>, we only need to modify the

nonlinear function in the main program to the proposed sine function, which is the named Fast-ICA(sin) algorithm in Table 1. There are four nonlinear functions involved in the comparison: three commonly used $g_1(\cdot)$, $g_2(\cdot)$ and $g_3(\cdot)$ in equation (3), and $g_4(\cdot)$ proposed in this paper.

The simulations were repeated and averaged to obtain the average correlation coefficient and running time in order to avoid randomness and improve the reliability of results. The number of iterations was set to 20. The average correlation coefficient is computed between the separated signal and the source signal, and the average running time is computed for each program (unit: seconds) [7, 8].

Simulation 1. In this simulation, the image signal, communication signal, and sound signal were used as the source signal [4].

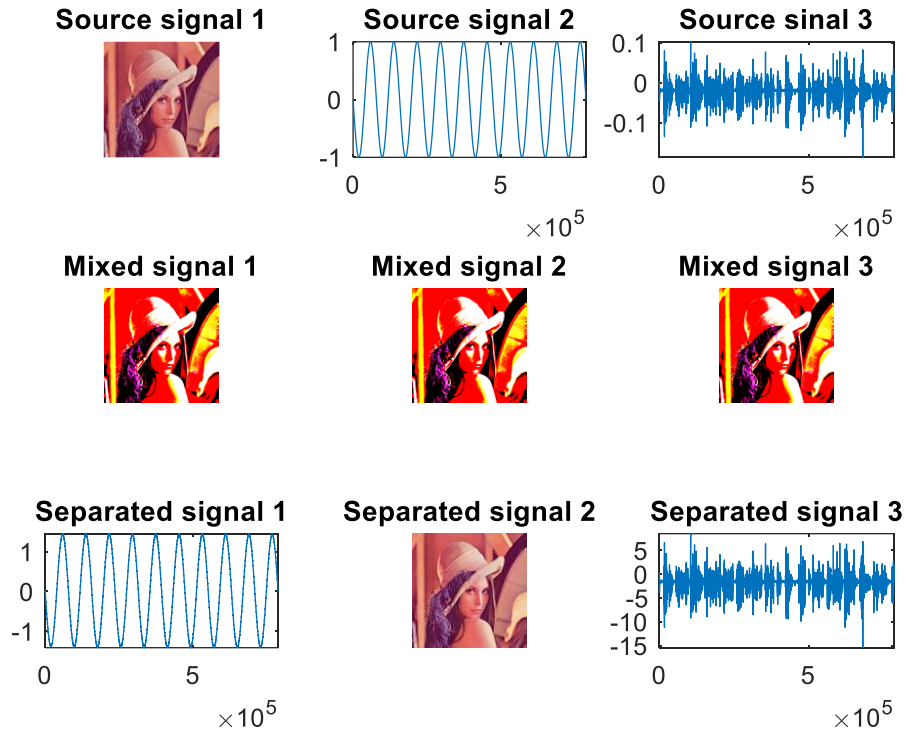


Fig. 2 – Separation results of Fast-ICA(sin) algorithm.

The widely used test image 'lenna.bmp' was adopted as the image source signal, of which size is 512×512 , and the bit depth of the image is 24. The common sine wave signal was used for the signal of the communication source. Music tune, 'guitar.wav,' was used for sound source signal. The signal to separate consisted of the mixed sub-Gaussian signal and the super-Gaussian signal. The separation results of the Fast-ICA(sin) algorithm are shown in Fig. 2, providing a promising separation ability.

The separation accuracy and computational times are compared with different nonlinear functions of the Fast-ICA algorithm. The average correlation coefficient (C-ave) and the average running time (T-ave) were computed on 20 repetitions and summarized in Table 2, which shows that the proposed nonlinear function 'sin' achieves comparable separation accuracy but outperforming computation speed (in bold text).

Table 2

Average correlation coefficient and average running time

non-linearities	C-ave	T-ave (s)
'tanh'	0.9984	0.9154
'gauss'	0.9986	0.8855
'pow3'	0.9991	1.2037
'sin'	0.9992	0.8038

Simulation 2. In this simulation, we used two linear frequency modulated (LFM) source signals, also known as chirp signal [9], whose spectrum is overlapped. It is widely used in communication, radar, sonar, biomedical, and seismic exploration systems. The source signals were separated by LFM signals with different bandwidths. Here, the number of source signals was set to 3, the number of observation signals was also set to 3, and the number of sampling points L was taken as 100. The separation results of the Fast-ICA(sin) algorithm are shown in Figure 3. As shown in Figure 3, the Fast-ICA (sin) algorithm could effectively separate the source signal from the three mixed LFM signals.

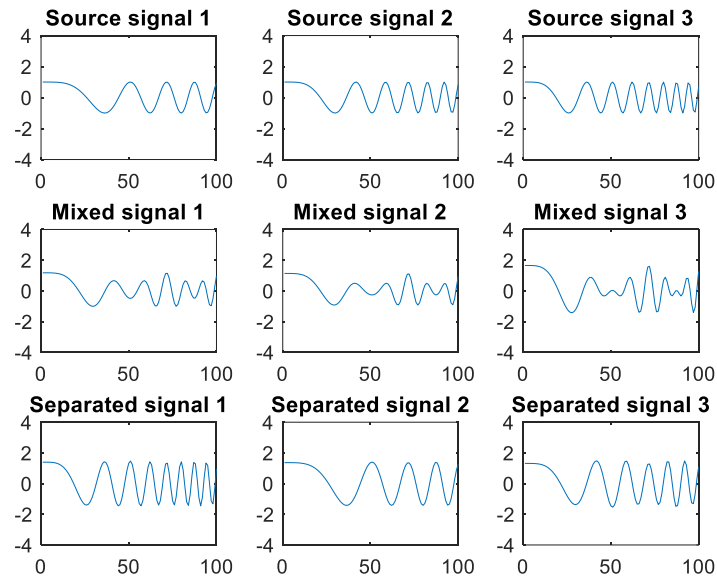


Fig. 3 – Separation results of Fast-ICA(sin) algorithm.

We further studied the performance of the algorithm according to the number of sources increases.

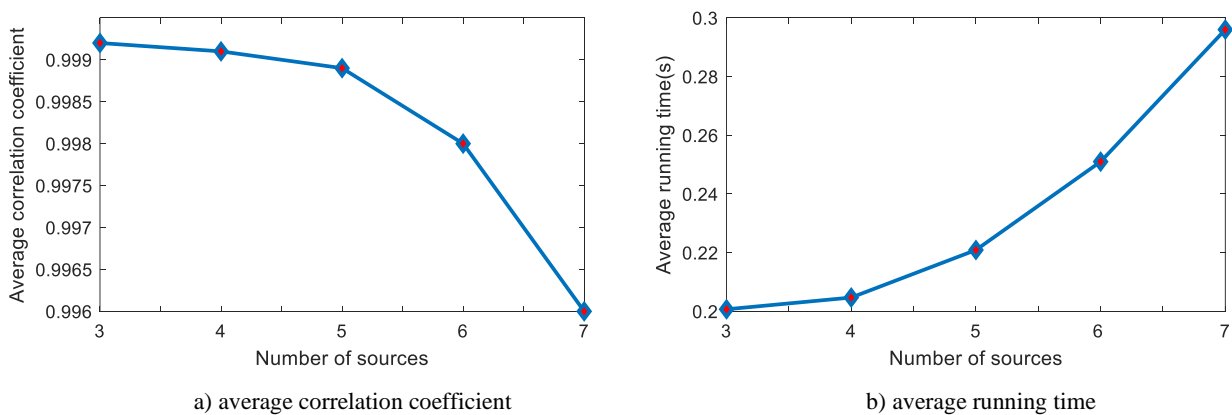


Fig. 4 – Separation performance according to the number of sources.

The LFM signals with different bandwidths were used as source signals. The number of sources increased from 3 to 7. The signal-to-noise ratio (SNR) in the additive white gaussian noise (AWGN) channel was set to 60dB [10, 11]. The mixed matrix A was generated randomly, and accordingly, 100 samples of the source signal were generated. The average correlation coefficient and average running time were computed on 20 repeated simulations. Figure 4 shows the separation performance according to the number of sources. As shown in Fig. 4, the average correlation coefficient decreases, and the average running time increases with the increased number of source signals. That is, the separation performance decreases as the number of source signals increases.

4. CONCLUSION

The negative entropy-based Fast-ICA algorithm requires selecting a proper nonlinear function according to the non-Gaussian property of the source signal. In this paper, we show the rationality of the sine function as a nonlinear function in three aspects and prove its convergence. Then, the separation ability of the proposed Fast-ICA (sin) algorithm is validated on the image signal, communication signal, and sound signal. Also, taking the LFM signal as an example, the separation effect is analyzed according to the increased number of source signals. Test of actual communication signals needs further study and discussion.

ACKNOWLEDGMENTS

This work was partially supported by the project of industrial-academic-research cooperation of Jiangsu province (No.BY2020241), qing lan project of Jiangsu province and opening project of Henan Engineering Laboratory of Photoelectric Sensor and Intelligent Measurement and Control (No.HELPSIMC-2020-002).

REFERENCES

1. P. XU, Y. JIA, M. JIANG, *Blind audio source separation based on a new system model and the savitzky-golay filter*, Journal of Electrical Engineering, **72**, 5, pp. 1–5, 2021.
2. A. HYVARINEN, E. OJA, *A fast fixed-point algorithm for independent component analysis*, Neural Computation, **9**, 7, pp. 1483–1492, 1997.
3. A. HYVARINEN, *Fast and robust fixed-point algorithms for independent component analysis*, IEEE Transactions on Neural Networks, **10**, 5, pp. 626–634, 1999.
4. P. XU, Y. JIA, *Blind source separation based on source number estimation and fast-ICA with a novel non-linear function*. Proceedings of the Romanian Academy, Series A, **21**, 4, pp. 93–194, 2020.
5. A. HYVARINEN, J. KARHUNEN, E. OJA, *Independent component analysis*, Wiley Interscience, New York, 2001.
6. Q. MA, J. YE, *Convergence and consistency analysis of fastICA algorithm*, Computer Engineering and Applications, **56**, 4, pp. 35–41, 2020.
7. P. XU, Y. JIA, Z. WANG, M. JIANG, *Underdetermined blind source separation for sparse signals based on the law of large numbers and minimum intersection angle rule*, Circuits, Systems, and Signal Processing, **39**, 5, pp. 2442–2458, 2020.
8. Y. JIA, P. XU, *Convolutional blind source separation for communication signals based on the sliding Z-transform*, IEEE Access, **8**, pp. 41213–41219, 2020.
9. P. XU, Y. JIA, *Blind source separation for chirp signals based on the local quadratic regression smoothing*, Comptes Rendus de l'Académie Bulgare des Sciences, **73**, 11, 1579–1585, 2020.
10. Y. JIA, P. XU, Z. WANG, P. ZONG, *Blind source separation of rotor vibration signals in high-noise environments*, Revista Internacional de Métodos Numéricos para Cálculo y Diseño en Ingeniería, **37**, 7, pp. 1–7, 2021.
11. Y. JIA, P. XU, *Noise cancellation in vibration signals using an oversampling and two-stage autocorrelation model*, Results in Engineering, **6**, p. 100136, 2020.

Received May 1, 2021